Journal of Structural Biology 192 (2015) 392–402

Contents lists available at ScienceDirect

Journal of Structural Biology

journal homepage: www.elsevier.com/locate/yjsbi

The giant keyhole limpet radular teeth: A naturally-grown harvest machine

Tina Ukmar-Godec [a,b,*], Gregor Kapun [b], Paul Zaslansky [c], Damien Faivre [a]

[a] Department of Biomaterials, Max Planck Institute of Colloids and Interfaces, Research Campus Golm, 14424 Potsdam, Germany
[b] Laboratory for Materials Chemistry, National Institute of Chemistry, 1000 Ljubljana, Slovenia
[c] Charite, Berlin Brandenburg Center for Regenerative Therapies, Julius Wolff Institute, 13353 Berlin, Germany

ARTICLE INFO

Article history:
Received 20 May 2015
Received in revised form 21 September 2015
Accepted 30 September 2015
Available online 3 October 2015

Keywords:
Giant keyhole limpet
Megathura crenulata
Rhipidoglossan radula
Electron microscopy
Amino acid analysis
X-ray scattering
Micro-CT

ABSTRACT

The limpet radula is a feeding organ, which contains more than 100 rows of teeth. During their growth the teeth mature and advance in position along the radula. The simpler doccoglossan radulae operate by grinding rocky substrates, extracting the algae by rasping and scraping with the teeth functioning as shovels. Less is known about the rhipidoglossan radulae, used as rakes or brooms that brush and collect loose marine debris. This type of radula is found in the giant keyhole limpet (*Megathura crenulata*). The large size of this organism suggests that the rhipidoglossan radula entails a technological superiority for *M. crenulata* in its habitat. The structure and function of the radulae teeth have however not been reported in detail. Using a combination of 2D and 3D microscopy techniques coupled with amino acid analysis and X-ray scattering, we reveal the working components of *M. crenulata*'s radula. It is characterized by numerous marginal teeth surrounding a pair of major hook-like lateral teeth, two pairs of minor lateral teeth and a large central tooth. The mature major lateral teeth show pronounced signs of wear, which gradually increase towards the very front end of the radula and are evidence for scraping. An abrupt change in the amino acid composition in the major lateral teeth and the concurrent formation of a chitinous fiber-network mark the onset of tooth maturation. In comparison to the simpler rock-scraping doccoglossate limpets, the radula of *M. crenulata* forms an elaborate feeding apparatus, which can be seen as a natural harvest machine.

1. Introduction

The radula is a unique feeding apparatus specific to mollusks. It is an elongated flexible membrane to which numerous teeth are anchored (Cruz and Farina, 2005; Rinkevich, 1993; Runham et al., 1969; Shaw et al., 2008). The radular teeth are used to graze or cut food (algae, detritus, plants or even animals) as the membrane is manipulated by various muscles and cartilages (Guralnick and Smith, 1999). There exist seven basic types of radula morphology, considered by some to reflect the various stages in the evolution from carnivorous to herbivorous feeding habits of the different mollusks (Steneck and Watling, 1982). Herbivorous mollusks that graze for algae need more teeth with different functions to scrape, grind and brush the food from the substrate to which they attach (Steneck and Watling, 1982). Limpets (Mollusca, Gastropoda) are a large group of primitive marine mollusks characterized by their inverted cone-shaped shells. They mostly inhabit intertidal zones but are also found in deep-sea hydrothermal vent sites (Cruz and Farina, 2005). The limpet radula is a toothed structure (Fig. 1), which contains more than 100 rows of teeth of various kinds, but only the outermost few rows are actively used at any given time (Lowenstam and Weiner, 1989). During their growth and maturation, the teeth advance in position along the radula in a conveyor belt manner and eventually enter the scraping zone, i.e. the front end of the radula, which is in contact with the substrate while feeding (Lowenstam and Weiner, 1989). Once the teeth start to function, they begin to wear down until they are discarded, at an average rate of one tooth row per day (Kirschvink and Lowenstam, 1979). At the same time, a new row of teeth emerges (Isarankura and Runham, 1968; Shaw et al., 2008). Limpets are predominantly herbivorous and their radular morphology is either doccoglossan or rhipidoglossan (see schematic in Fig. 2) (Goldberg, 2013). The doccoglossan ('docco' is the Latin word for beam and 'glossa' for tongue) radula (Fig. 2, left panel) is structurally rather primitive, with only two types of teeth (marginal and lateral), whereas the rhipidoglossan ('rhipido' is the Latin word for fan)

* Corresponding author at: Department of Biomaterials, Max Planck Institute of Colloids and Interfaces, Research Campus Golm, 14424 Potsdam, Germany.
E-mail address: Tina.UkmarGodec@mpikg.mpg.de (T. Ukmar-Godec).

http://dx.doi.org/10.1016/j.jsb.2015.09.021
1047-8477/

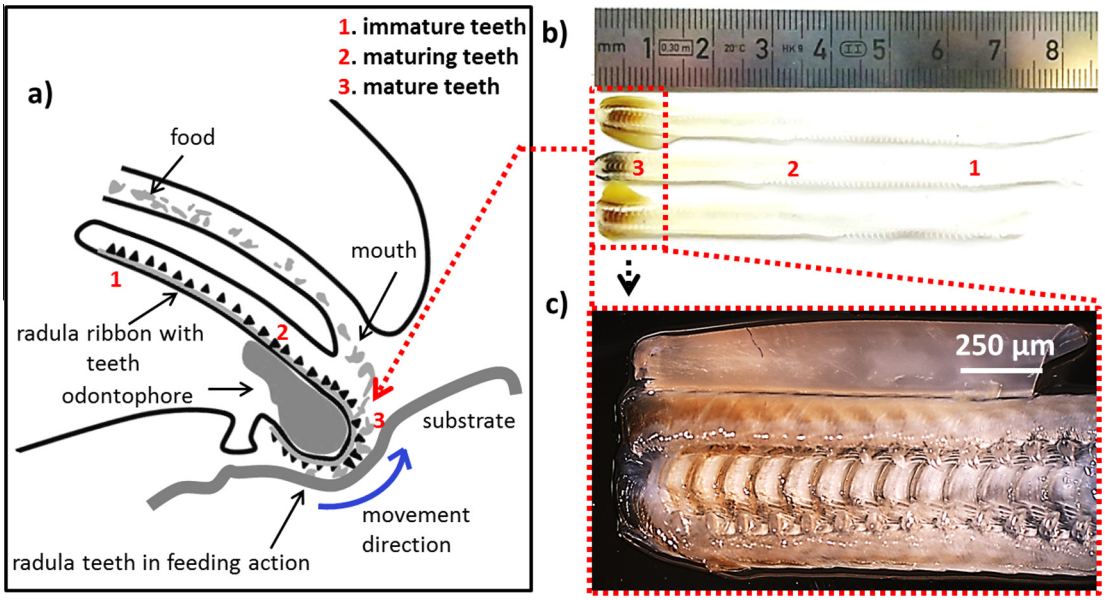

Fig. 1. (a) Schematic of the limpet radula in feeding action. The blue arrow denotes the direction of radula movement during the stroke. (b) A photograph of extracted radula of three adult giant keyhole limpets depicting the inter-specimen variability. (c) Optical micrograph of the mature end of the radula.

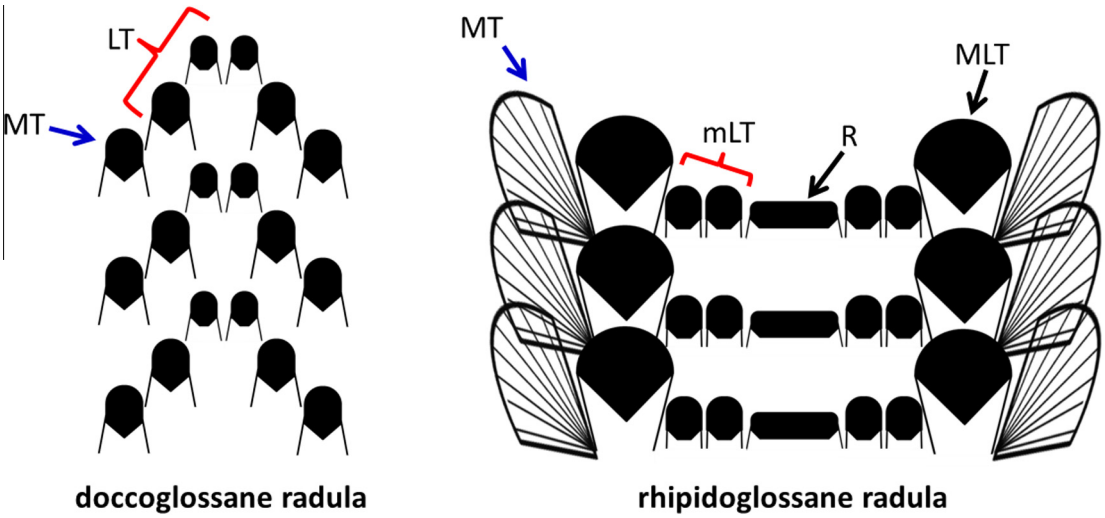

Fig. 2. Schematic representations of the two major types of herbivorous limpet radulae: (left) doccoglossane radula and (right) rhipidoglossane radula. The abbreviations denoting various teeth are: MT = marginal teeth, LT = lateral teeth, mLT = minor lateral teeth, MLT = major lateral teeth and R = central or rachidian tooth.

radula (Fig. 2, right panel) has a variety of different teeth (marginal, two types of lateral and central).

In the doccoglossan radula (Fig. 2, left panel), there is typically a small central tooth, up to three lateral teeth and up to 3 marginal teeth in each row (Steneck and Watling, 1982). In some doccoglossate species, the central tooth is missing. The teeth are stiff and fixed, and of limited mobility due to the low number of radula muscles (Steneck and Watling, 1982). Doccoglossate radulae are found in the earliest limpets (families Patellidae, Lottiidae, Lepetidae) and function like chains of shovels scraping hardened macroalgae (Cruz and Farina, 2005; Isarankura and Runham, 1968; Kirschvink and Lowenstam, 1979; Lowenstam and Weiner, 1989; Shaw et al., 2008; Steneck and Watling, 1982). The large spaces between the teeth are not suitable for collecting microalgae from substrates (Steneck and Watling, 1982), such that the doccoglossate limpets are less adaptable to different food resources, i.e. they are limited to feeding on larger algae. These early limpet families have mineralized teeth, containing either crystalline goethite and silica (in shallow-water limpets (Faivre and Ukmar Godec, 2015; Grime et al., 1985; Lowenstam, 1962; Lowenstam, 1971; Sone et al., 2005; Sone et al., 2007; Towe and Lowenstam, 1967; van der Wal, 1989)) or amorphous silica and amorphous iron oxide (in the deep-sea hydrothermal vent limpet (Cruz and Farina, 2005)). The combined effects of mineralized teeth on a rigid radula give rise to an enhanced stroke with impressive excavating ability of doccoglossate limpets whilst feeding (Steneck and Watling, 1982). The mineral fiber length in the doccoglossate limpet teeth was suggested to be optimized to ensure maximal efficiency during mechanical loading (Lu and Barber, 2012). Doccoglossate limpet teeth were found to have an absolute material tensile strength that is the highest recorded for a biological material (Barber et al., 2015).

The more advanced so-called rhipidoglossan radula, depicted schematically in Fig. 2 (right), is found in all archeogastropods except in true limpets (Steneck and Watling, 1982) and is the most complex and structurally sophisticated among the radulae of herbivorous mollusks. It contains numerous different teeth per row and a myriad of muscles in the buccal mass (Graham, 1973). In striking contrast to the doccoglossate limpets the rhipidoglossane limpet teeth are not mineralized with iron compounds (Goldberg, 2013; Steneck and Watling, 1982). Most of the muscles can create minor adjustments of tension and position of the radula ribbon, which splays the numerous marginal teeth during the protraction strokes of the radula (Steneck and Watling, 1982). The marginal teeth and the more massive lateral teeth are very long as compared to their overall length (see right panel in Fig. 2) and the teeth have relatively narrow bases attaching them to the radular membrane. Consequently while in function, it is sufficient to induce a small change in the tension applied to the radular membrane, to effect an extensive movement of the distal tips of the teeth (Steneck and Watling, 1982). Collecting the food is assumed to be mostly accomplished by the major lateral and the marginal teeth, whereas the central tooth is thought to be less involved in this process (Fretter and Graham, 1962). Because the marginal teeth are typically very long and the lateral teeth are not mineralized, these radulae operate like brooms, typically collecting the softer microalgae and only rarely feeding on the somewhat tougher leathery macrophytes (Steneck and Watling, 1982). The complex and well controlled protraction motion of the radular membrane give rise to sweeps, effectively collecting algae with a variety of sizes. Larger rhipidoglossate gastropods are able to remove the tougher cortical algal cells (Steneck and Watling, 1982).

The giant keyhole limpet *Megathura crenulata* (*Mcren*) is a rhipidoglossate limpet, certainly the largest known member of its species, as the name indicates: *Mcren* can reach up to 13 cm in length. This species inhabits the rocky reefs of the eastern Pacific of the North American coast (Morris et al., 1980). In California *Mcren* is important economically, because it produces the extracellular protein hemocyanin, a product used in immunology and oncology (Beninger et al., 2001; Harris and Markl, 2000; Martin et al., 2011; Martin et al., 2007; Mazariegos-Villarreal et al., 2013). *Mcren* differs from typical rhipidoglossate gastropods as it is an omnivorous gastropod, feeding on both red and brown algae as well as on tunicates (Beninger et al., 2001; Harris and Markl, 2000; Martin et al., 2011; Martin et al., 2007; Mazariegos-Villarreal et al., 2013; Morris et al., 1980). A dominant portion of its diet consists of red algae *Coralina* although hard articulated calcareous algae such as *Coralina* are typical docoglossate limpet food. Thus, *Mcren* has found a way to ingest calcareous algae considered to be too hard for the radulae of other rhipidoglossate gastropods (Steneck and Watling, 1982). The feeding strategy of *Mcren* thus presumably differs from both the simpler scraping limpets as well as the more evolved sweeping rhipidoglossan mollusks. *Mcren* combines sweeping 'knowhow' of rhipidoglossan radulae (Fretter and Graham, 1962; Graham, 1973; Steneck and Watling, 1982) with a high scraping efficiency (Cruz and Farina, 2005; Grime et al., 1985; Lowenstam, 1962; Lowenstam, 1971; Steneck and Watling, 1982; Towe and Lowenstam, 1967; van der Wal, 1989) and appears to have evolved an advanced, multi-use harvest machine, which has not been described so far.

Here, using optical and scanning electron microscopy (SEM) combined with laboratory X-ray micro-computed tomography (μCT), X-ray scattering and amino acid analysis to report on the anatomy and development characteristics of the radula of *Mcren*. We describe the morphological changes and the evolution of the protein composition in the radular teeth during their evolution from immature to the mature fully-functional structures.

2. Material and methods

2.1. Limpet sample preparation

Limpets were purchased from the Monterey Abalone Company (California, USA). The radulae were extracted from *Mcren*, placed on petri dishes in order to preserve a flat shape and immediately transferred to a freezer at −80 °C until further use. For the analyses reported here, freshly defrosted radulae were thoroughly washed in 3 steps in order to remove all organic debris: (i) washed in water and gently brushed with an ultra-soft brush, (ii) immersed shortly in 1% SDS and (iii) washed again in water.

2.2. Sample embedding and polishing

Mature radula sections were dehydrated by a series of increasing ethanol concentrations (30%, 50%, 70%, 80%, 90% and 100%) and embedded in polymethylmethacrylate (PMMA). The embedded samples were cut with a slow speed saw (Bühler Isomet Low Speed Cutter 1000), ground with silicon carbide paper of increasing grit sizes and finally polished using 3 and 1 μm particulate diamond slurries.

2.3. Optical microscopy

Optical images of segments of the radula containing teeth of varying maturity were obtained using a light microscope equipped with a digital camera (Leica DM RXA2 with CCD camera). The mature end of the radula was additionally imaged with a second lower magnification light microscope with a larger field of view (Leica M165 C with KL 1500 LCD illuminator) to fit the entire end of the radula.

2.4. Scanning electron microscopy (SEM)

SEM micrographs of the immature, maturing and mature sections of a dry radula were obtained using two SEM instruments: (a) Field emission SEM (FE-SEM, Supra35 VP, Carl Zeiss, Germany) operating at 3 kV, 5 kV and 10 kV; (b) high-resolution SEM (HR-SEM, JEOL JSM7500F) operating at 5 kV. The samples were mounted on an SEM-sample holder with conductive carbon tape and sputtered with Pt.

2.5. Inductively coupled plasma-optical emission spectrometry (ICP-OES)

The Fe content in major lateral teeth was determined using ICP-OES Optima 8000 (Perkin Elmer). Major lateral teeth were extracted from the front (colored), middle and back (immature) parts of the radula. The extracted teeth were first placed in 0.5 ml of aqua regia (167 μl HNO_3 + 333 μl HCl) and heated at 40 °C overnight in order to achieve a better dissolution. Afterwards the samples were diluted with 3.5 ml of water (DDW) and subsequently the Fe content measured with ICP-OES. The apparatus was calibrated for Fe with ICP Multi-Element Standard Solution (Carl Roth, 28 elements in 5% nitric acid, 100 mg/l) and with an external standard with ICP Multi-Element Standard Solution (Carl Roth, 22 elements in 5% nitric acid, 1 mg/l). Measurements were performed on major lateral teeth from 3 different radula samples.

2.6. Micro-computed tomography (μ-CT)

Samples of mature teeth were imaged using a laboratory microCT (Skyscan 1172 lab CT, BrukerCT, Kontich, Belgium). Scans were performed using 50 keV, with an effective pixel size of 2 μm,

0.7 s exposure time. The data was reconstructed into isotropic voxels using the standard manufacturer reconstruction package (Nrecon, BrukerCT, Kontich, Belgium) and the reconstructed volumes were visualized in 2D (Fiji (Schindelin et al., 2012)) and in 3D (CTvox 2.6, BrukerCt, Belgium and Amira 5.2, Visage Imaging GmbH, Germany).

2.7. Amino acid analysis (AAA)

The amino acid composition of the proteins comprising the teeth of different states of maturity was determined by Genaxxon bioscience GmbH using an amino acid analyser LC3000 on non-embedded samples. Five teeth of each stage of maturity were extracted with tweezers and gently air-dried. Each sample was transferred into a hydrolysis glass tube and lyophilized prior to any further processing. The lyophilized samples were treated with HCl (700 μL 6 N), sealed under vacuum ($p < 20$ mbar) and hydrolyzed for 60 h at 110 °C. After hydrolysis, the samples were dried at 36 °C for 8 h (vacuum centrifuge). Each dried sample was immersed in a Na-acetate buffer (500 μL, pH 2.2) for subsequent derivatization and high pressure liquid chromatography (HPLC; polymeric cation exchange column). Fragmented amino acids were detected by post-column Ninhydrin derivatization at 125 °C and photometric measurement at 570 nm (due to high Glycine (Gly) content Gly was determined at 440 nm). Data was monitored by the chromatography software ChromStar 6.0 following calibration of the HPLC using a commercial standard (Sigma–Aldrich, A2908). The calibration was performed prior to the evaluation of each sample.

2.8. Synchrotron-based X-ray scattering

X-ray scattering experiments were performed on the embedded thin samples at the mySpot beamline (Paris et al., 2007) at the BESSY II synchrotron radiation facility in Berlin (Germany). A beam energy of 15 keV ($\lambda = 0.826$ nm) was defined using a multilayer monochromator. The beam was focused by a toroidal mirror and experiments were collected on the area detector (MarCCD 225, MarUSA, Evanston) situated approximately 325 mm away from the sample. The final beam size was defined by a pinhole of 30 μm diameter behind the sample. All measurements were calibrated using a quartz powder placed at the sample position. The software DPDAK (Benecke et al., 2014) was used for the analysis of the 2-dimensional scattering data. The total scattering intensities of the (040) and (013) reflections were used to determine the relative chitin content (Seidel et al., 2008). The difference in the results obtained from both reflections was within the statistical error.

3. Results

3.1. Mature teeth morphology and the radular tooth formula

Optical micrographs of representative extracted radula specimens are shown in Fig. 1b. The radula of a typical *Mcren* adult specimen is about 8 cm long and 0.5 cm wide. The color of the radula turns gradually from white in the immature end towards a brownish color at the mature end (see magnification in Fig. 1c). The intensity of the color varies somewhat between the species and does not appear to be correlated with the specimen size or the radula length. The observed coloration might be due to protein sclerotization (Rubin et al., 2010) or due to the presence of Fe or a combination of both. To test for the presence of Fe we performed ICP-OES. The average Fe concentrations in solutions of dissolved major lateral teeth determined using ICP-OED are 0.273 ± 0.093 mg L^{-1} in the front-most and colored part, 0.074 ± 0.032 mg L^{-1} in the maturing region and 0.071 ± 0.045 mg L^{-1} in the immature region. It should be noted that the limit of detection of the experiment as determined by measuring a blank sample was 0.06 mg L^{-1}. Therefore the coloration appears to be correlated with the presence of Fe in the teeth.

Optical and SEM micrographs of the mature end of the radula are shown in Figs. 3 and 4. The outer, brush-like structures are numerous marginal teeth (see Fig. 3a and c and compare with MT in Fig. 2 as well as with magnifications in Fig. 4g). The very high aspect ratio is likely the reason for their high flexibility. The marginal teeth have a characteristic appearance with small hair-like structures covering the tooth surface (see inset of Fig. 4g). Inwards from the marginal teeth on each side, we observe a major hook-like dicuspid lateral tooth (compare with MLT in Fig. 2 and see Fig. 3a and c along with Fig. 4a–d). The tooth base anchors the tooth cusp to the radular membrane (Fig. 4b and d). The bases of consecutive major lateral teeth interlock, which probably enhances the stability and rigidity during scraping (see Fig. 4b and d). The tooth side facing the direction of scraping is termed the anterior or "leading side" and the side facing in the opposite direction is called the posterior or "trailing side" (Fig. 4d). In the center of the radula, we observe a broad central tooth (also called rachidian tooth, denoted by R) (Khanna and Yadav, 2004) enclosed by four small unicuspid lateral teeth, of which the outer pair appears to be less developed (see Figs. 3b and 4e and f). The position and orientation of the rachidian tooth in the radula is depicted in the longitudinal cross-section Fig. 4f.

The radular tooth formula of *Mcren* is: $\infty + D + 4 + R + 4 + D + \infty$ where the central rachidian tooth (R) is enclosed with 4 minor lateral teeth, a dominant major lateral tooth (D) and a large number (∞) of marginal teeth.

A μCT image of a mature part of the radula is displayed in Fig. 4a and readily shows the dominant major dicuspid lateral teeth. The marginal teeth appear as brushes on both sides of the radula. We observe the size of mature major lateral teeth in a stage mostly unaffected by wear (see Fig. 5 and compare to the cusp length and sharpness in Fig. 9). This can be explained by the fact, that supply of new teeth is a controlled by the radular growth and not the dynamics of tooth wear (van der Wal et al., 2000). This in turn means, that the front-most lying mature teeth have been scraping over a longer period and are hence more extensively worn. In addition, the front most part of the radula is curved upwards, suggesting that the late-mature teeth face the substrate at different angles and are exposed to different stresses than the teeth in the mid- and early-mature phase (see Fig. 1a). The typical separation between the lowest part of the base and the tooth tip is about 1.2 mm. The length of the tooth cups is almost 1 mm and the width of the widest part of the cusp is 0.95 mm. Thus the length of major lateral teeth of *Mcren* is about 4–5 times larger than the length of typical doccoglossate limpets such as *Patella vulgata* (Jones et al., 1935; Mann et al., 1986; Runham, 1962; Runham et al., 1969) and *Patella caerulea* (Sone et al., 2005; Sone et al., 2007). Note the variation of the width along the tooth axis, which in *Mcren* (see central panel in Fig. 5) is much more pronounced than in the simpler scraping limpets (Jones et al., 1935; Mann et al., 1986; Runham, 1962; Runham et al., 1969; Sone et al., 2005; Sone et al., 2007). In particular, the ratio maximal width/tip length of ≈ 1 is much larger than in scraping limpets (Jones et al., 1935; Mann et al., 1986; Runham, 1962; Runham et al., 1969; Sone et al., 2005; Sone et al., 2007).

3.2. The development of major lateral teeth

Fig. 6 shows SEM and optical micrographs of the radula in the immature, maturing and mature regions. In the immature stage,

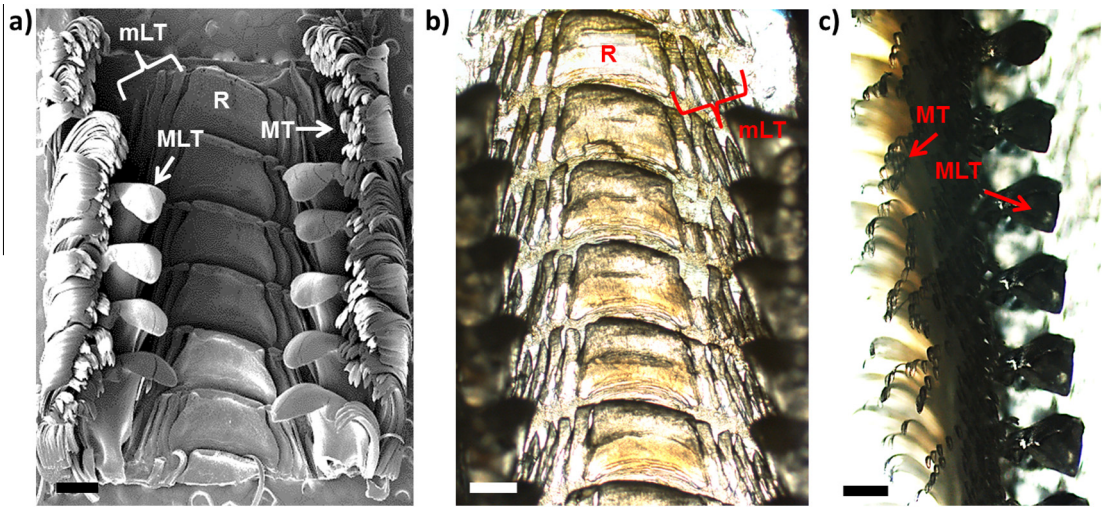

Fig. 3. (a) SEM micrograph of the mature end of the *Mcren* rhipidoglossan radula (compare with schematic in Fig. 2). The major lateral teeth in the first few rows are missing. (b) Optical micrograph of the mature region of the radula focusing on the large R tooth and mLT. (c) Optical micrograph of the mature region of the radula focusing on MLT. (a–c) abbreviated same as in Fig. 2. The scale bars correspond to 500 μm.

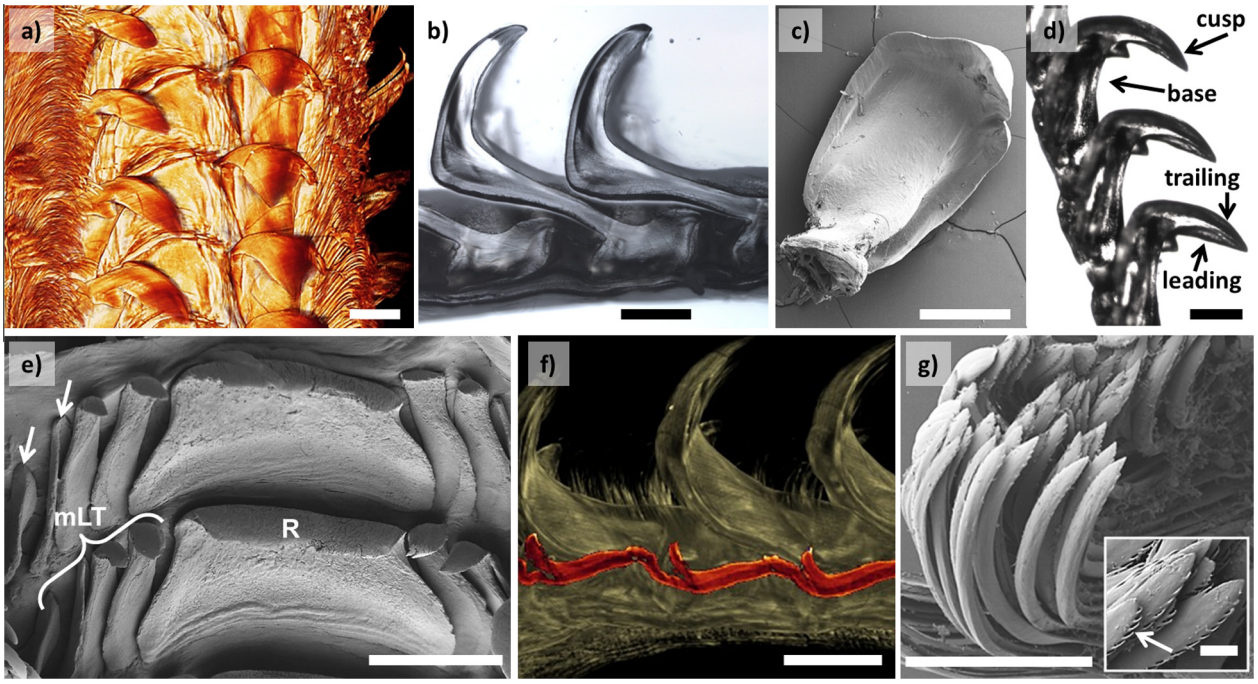

Fig. 4. (a) μCT image of the mature end of the radula. (b) Longitudinal section of two consecutive mature major lateral teeth. (c) SEM micrograph of an extracted mature major lateral tooth. (d) Optical micrograph of an extracted row of inter-locked mature major lateral teeth. (e) SEM micrograph of a mature R tooth enclosed by 4 unicuspid mLT. The arrows point at the two external underdeveloped mLT (abbreviated same as in Fig. 2). (f) μCT images of a longitudinal cross-section of the mature end of radula with the central tooth marked in red. (g) SEM micrograph of mature marginal teeth. Inset: a magnification depicting smaller hair-like structures (denoted by the arrow) covering the surface of marginal teeth. The scale bars in (a–g) are all 500 μm. The scale bar in the inset of (g) is 50 μm. The scale bar in the μCT image (a) is used as a guide to the eye.

all teeth are significantly smaller (see Fig. 6a and d). Compared to the mature stage, in the immature stage the marginal teeth are less densely packed and the central as well as minor lateral teeth are thinner (compare Fig. 6a and d with b, c and e and f). During the maturation process all teeth gain in thickness. The most extensive changes are observed in the development of the major lateral tooth (marked in red in Fig. 6a and b). Based on these changes we clearly delimit the immature from the maturing teeth. In the immature stage, the inter-locking of consecutive bases, in the sense that each base encloses the previous one, is less pronounced (Fig. 6a and d). The hook-like tooth cusp is oriented parallel to the radula axis, whereas in immature teeth it is oriented anti-parallel to the radula growth axis (compare Fig. 6a with b). At rows 15–20, the cusp orientation gradually changes from parallel to anti-parallel with respect to the radula growth (Fig. 6e). This transition typically occurs within 4–5 rows. In the maturing part of the radula (Fig. 6b and e), the tooth bases become thicker and a more pronounced inter-locking of bases is seen. The tips of the teeth still appear to be thinner and underdeveloped with respect to the mature stage. The transition from the maturing to the mature stage is not as clear as the one between immature and maturing stages. It is marked by a pronounced thickening of the tooth cusps and the

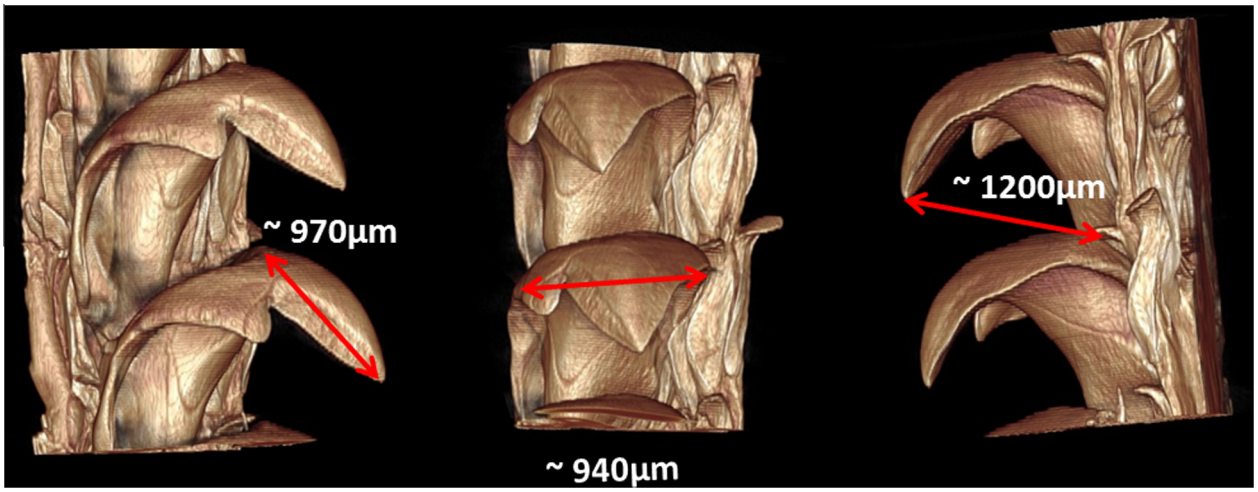

Fig. 5. A µCT image of a pair of consecutive major lateral dicuspid teeth from three different perspectives. Red arrows depict the measured distances.

development of a curved hook-like tip (see Fig. 6c and f). In the mature stage, the tooth cusps are initially longer than in the maturing stage but soon exhibit very pronounced signs of wear.

3.3. Amino acid analysis of the major lateral teeth

The amino acid (AA) analysis reveals marked differences in content as well as the AA composition of the proteins in teeth of various stages of maturity. We determined the total AA and glucosamine (GA) content expressed in $mol^{*}g^{-1}$ of tooth material as well as the respective relative content of different AAs. The total AA content in immature teeth is 165.24 $\mu mol^{*}g^{-1}$ and the respective AA composition is shown in Fig. 7. The AA composition in the immature stage is rather uniform with somewhat increased fractions of Glu (17%, comprising both Glu and Gln), Gly (16.45%), Asp (13.64%, comprising both Asp and Asn) and Ala (8.16%), whereas the remaining AAs are present in fractions of 2–6%. The content of GA, the building unit of chitin, is 161.6 $\mu mol^{*}g^{-1}$. The GA content corresponds to either the fraction of intrinsically free GA or to the easily hydrolysable chitin. In teeth in the maturing stage both the AA content and the AA composition change dramatically. The total AA content is 3.585 $mmol^{*}g^{-1}$ and thus more than 20 times larger than in immature teeth. The protein composition is strongly dominated by Gly (81.1%), His (10.3%) and Pro (5.74%), whereas the cumulative fraction of the remaining AA is about 2%. The GA content is 46.1 $\mu mol^{*}g^{-1}$, which is roughly four times lower than in the immature stage. In fully mature teeth the total AA content is 3.687 $mmol^{*}g^{-1}$ and hence very close to the AA content in maturing teeth. The AA composition is almost identical to the composition observed in the maturing stage, comprising Gly (82.1%), His (10%) and Pro (5.4%), whereas the cumulative fraction of the remaining AA is about 2.5%. The GA content in mature teeth is 47.6 $\mu mol^{*}g^{-1}$.

3.4. Chitin content and distribution in the major lateral teeth

Scattering experiments did not reveal any presence of chitin fibers in the immature teeth. In addition, they did not reveal the presence of any iron oxide nor other mineral phases. Diffractions signals arising from chitin fibers were found to appear instantaneously in the transition region between the immature and maturing teeth (see Fig. 6e). The local chitin content in the major lateral teeth is determined from the intensities of the (0 1 3) reflection and is depicted in Fig. 8. While the results do not allow for a quantification of the absolute chitin content, the intensities are normalized to a common scale and hence allow for a comparison of chitin concentrations between the samples. The largest chitin concentrations are observed in the anterior edge and continue towards the tip of the tooth. These are also the regions where significant chitin concentrations are observed first (Fig. 8a). In the posterior edge significant concentrations of chitin fibers are observed only in the mature stage (see results for a worn tooth in Fig. 8c).

3.5. Appearance of tooth wear

Optical and SEM micrographs of the major lateral tooth in the scraping zone are shown in Fig. 9 and exhibit a gradual increase in the degree of wear in terms of reduction in length and overall rounding of the shape of the tooth cusps.

Within a few rows, we observe a rather sharp change in the extent of wear. In total, *Mcren* wears down the major tooth cusp almost all the way to the kink of the cusp (see Fig. 9b and c). But even in completely worn teeth, showing pronounced traces of scraping activity, (compare Fig. 9d and f) the edge appears to be locally well preserved (see Fig. 9e). This observation is reminiscent of the so-called teeth self-sharpening effect observed in doccoglossate limpets (van der Wal, 1989) and sea urchins (Killian et al., 2011). In the SEM analysis we also observed that the worn teeth in the late mature stage developed cracks (Fig. 9d and e). This either suggests that the worn teeth develop cracks during feeding or that they become more brittle upon drying.

The developmental stages of the large central tooth during the maturation process are shown in Fig. 10. The immature tooth appears at first to be very thin. The front edge is typically curled, which could also be an artifact of drying. Already in the maturing stage, such a curl is not observed anymore, suggesting a marked change in the structural integrity of the tooth or its dependence of the degree of hydration.

As compared to the major lateral tooth, the surface of the large central tooth is much rougher and appears to be porous. Also, compared to the kinked major lateral tooth, the central tooth appears to have a more uniform radius of curvature (see Fig. 4f). In addition, µCT clearly revealed that the angle at which the edge is exposed to the substrate is different in the large central tooth as compared to the major lateral tooth (Fig. 4f), indicating that it may have a different operational mode. More specifically, the sharp edges – "the blades" – of the major lateral and central tooth are exposed to the substrate at different angles during a stroke of the radula. In the late mature developmental stages, the central tooth as well exhibits pronounced signs of wear (Fig. 10d).

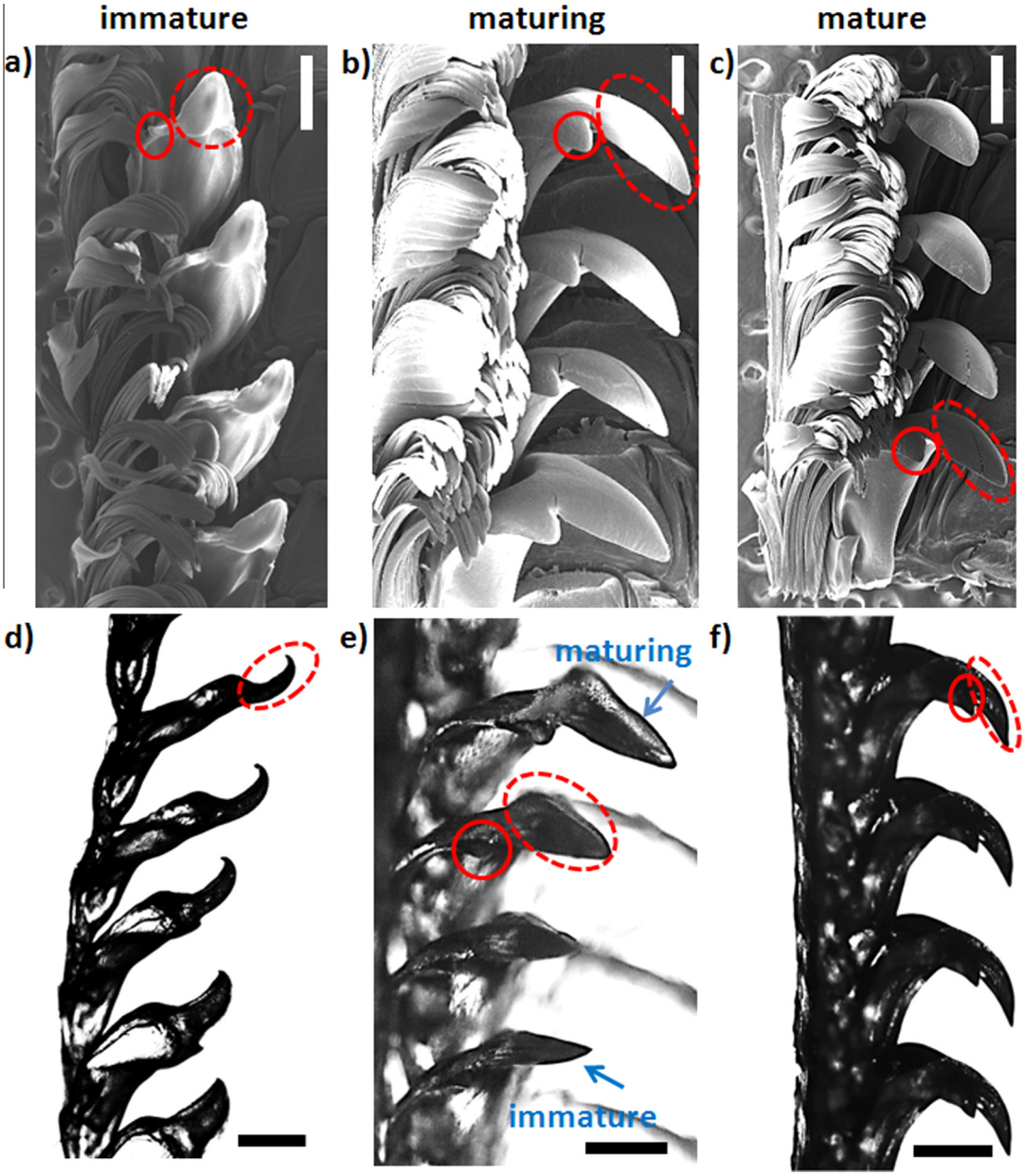

Fig. 6. SEM images of the (a) immature, (b) maturing and (c) mature part of the radula. (d and e) Optical micrographs of various stages of maturation of the major lateral tooth: (d) immature stage, (e) transition between immature and maturing and (f) mature stage of the teeth. The SEM and optical images correspond to different radulae, respectively. The red full and dashed circles denote the minor and major cusp of the dominant lateral tooth respectively. The scale bars are 500 μm.

4. Discussion

The main features of the *Mcren* radula agree with conventional descriptors of the rhipidoglossate gastropod radula. For instance, the numerous dense marginal teeth are conceivably very efficient in collecting small loosened remnants of algae. The major lateral teeth are very dominant and have hook-like shapes. The fact that the tooth is curved causes the largest stresses generated during feeding to concentrate near the cusp-base transition region (van der Wal et al., 2000). In doccoglossate limpets the tooth width first increases and shortly after remains constant in the direction towards the tooth base. While the contour of the tooth in *Mcren* near the tooth base is similar to the one in doccoglossate limpets, the tooth width afterwards increases more extensively and reaches a pronounced maximum at the apex of the hook, i.e. in the region, where stresses concentrate during a stroke (van der Wal et al., 2000). In turn this might be beneficial in the sense that it could represent a local mechanical reinforcement. Such a reinforcement might represent an evolutionary upgrade, which contributes to *Mcren*'s ability to harvest hard algae. Extensive signs of wear are evidence of intense scraping/cutting activity on hard substrates (such as red calcareous algae). The large central tooth exhibits pronounced signs of wear in contrast to the minor lateral as well as marginal teeth. A different orientation of the central tooth with respect to the major lateral teeth indicates that this tooth most likely acts like a knife, cutting or grinding the substrate. The signs of wear on the major lateral and central tooth contrast with the known rhipidoglossane mode of harvest where the marginal brooms act as the main operational teeth (Fretter and Graham, 1962). *Mcren* hence uses a multitude of different tools (hook-like shovels, knives and brooms) in the feeding process.

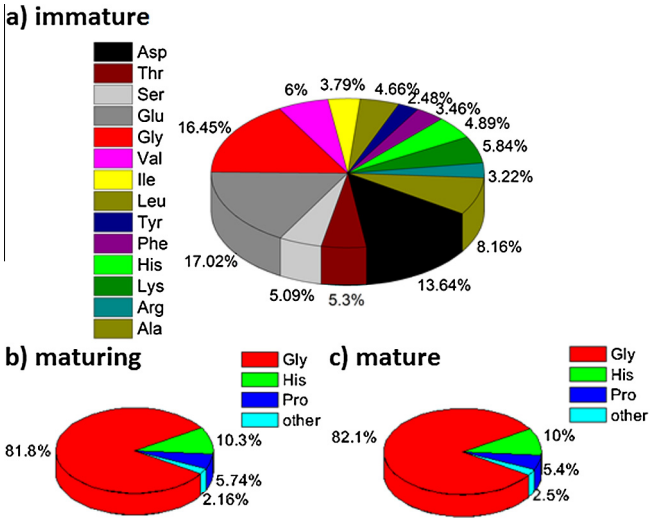

Fig. 7. The relative amino acid composition of proteins in (a) immature, (b) maturing and (c) mature teeth.

The brownish coloration of the front-most part of the radula might be connected to the presence of traces of Fe. Namely, ICP-OES measurements revealed observable Fe amounts only in the colored region, which contains predominantly substantially worn teeth. This observation suggests that the Fe originates from repeated contact with *Mcren's* food. Alternatively, or in addition to this, the coloration might appear due to protein sclerotization, which is frequently observed in non-mineralized biomaterials (Rubin et al., 2010) and remains to be analyzed in forthcoming work.

The changes accompanying tooth development during the maturation process suggest that *Mcren* first builds a soft scaffold for the teeth and afterwards gradually reinforces it. Note that this reinforcement does not follow the generic biomineralization strategies observed in doccoglossate limpets (Faivre and Ukmar Godec, 2015; Sone et al., 2007) as rhipidoglossan teeth lack the mineralization present in the doccoglossan radulae (Goldberg, 2013; Steneck and Watling, 1982). Instead, the reinforcement involves only chitin and proteins. The initially thin major lateral teeth gradually thicken and their tips gradually reorient from the direction parallel to the radula growth axis into the anti-parallel direction in the maturing stage. In this stage, the tooth cusp, and especially the tip of the tooth, becomes thicker. Accompanying these observations are also marked changes in the AA composition as well as in the GA content. The large drop in the GA content accompanying the transition from the immature to the maturing stage either indicates the formation of a complete chitinous network (resulting in less intrinsically free GA) or the presence of more compacted and less accessible chitin fibers, which are less susceptible to acid hydrolysis (Rupley, 1964). The X-ray scattering results fully support these observations. They further reveal that chitin reinforcement starts at the anterior edge and in the developing tooth at the transition between immature and early maturing teeth. In the mature stage, the posterior edge becomes reinforced with chitin fibers as well, but the relative content is lower than in the anterior edge. The abrupt change in the AA content and composition further implies that the proteins present during the formation of the chitinous scaffold are very different from those occurring in the maturing and mature stages, where the teeth become thicker. The AA composition in the latter stages is strongly dominated by Gly, His and Pro. Gly and Pro are generally abundant in fibrilar structural proteins such as collagen, elastin, titin and elastomeric and amyloid fibrils (a large Gly content gives rise to a high degree of helical structure and Pro is a structural disruptor and rigidifier) (Cheng et al., 2010; Rauscher et al., 2006; Yang et al., 2014). The high degree of hydrophobicity of proteins might also be responsible for a decreased susceptibility of chitin fibers to acid hydrolysis by making them less accessible to water. Moreover, the Gly and Pro composition is above the threshold in which amyloid formation is impeded and elastomeric properties become apparent (Rauscher et al., 2006). The Gly and His rich AA composition resembles the one of sclerotized structural proteins, which are mechanical reinforcement materials in some marine invertebrates (Rubin et al., 2010). This suggest that proteins could play an important role for the mechanical properties of the mature radular teeth of *Mcren* but further analyses are needed to obtain a definite answer.

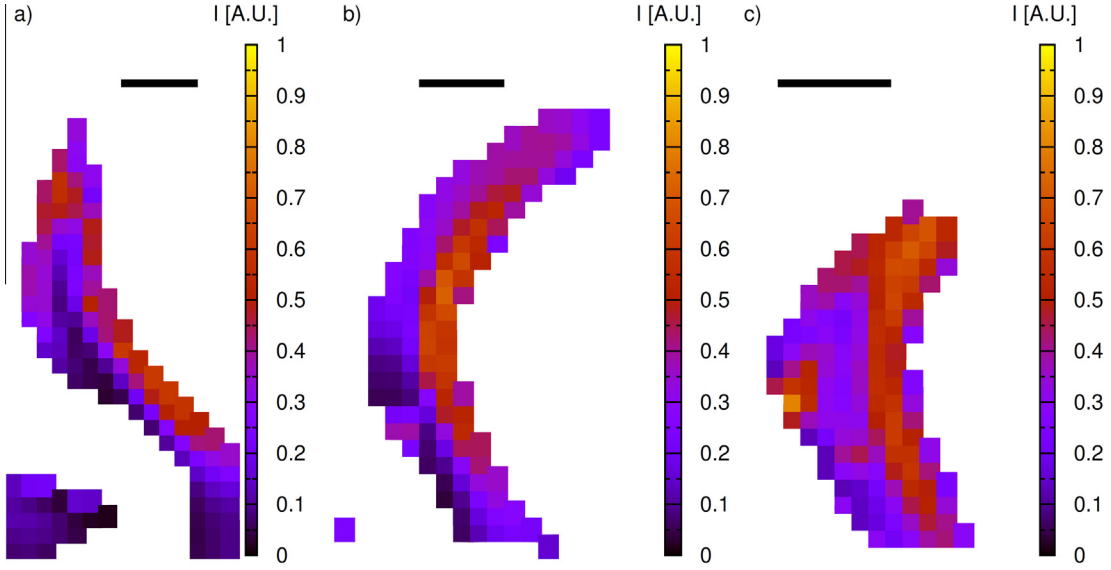

Fig. 8. Scattering intensity from the (013) reflection of α-chitin in major lateral teeth: (a) transition region between immature and maturing teeth (see Fig. 6e), (b) early mature tooth and (c) extensively worn mature tooth. The intensities in (a–c) are normalized to a common scale in order to allow for a relative comparison of the chitin content. The scale bar corresponds to 200 μm.

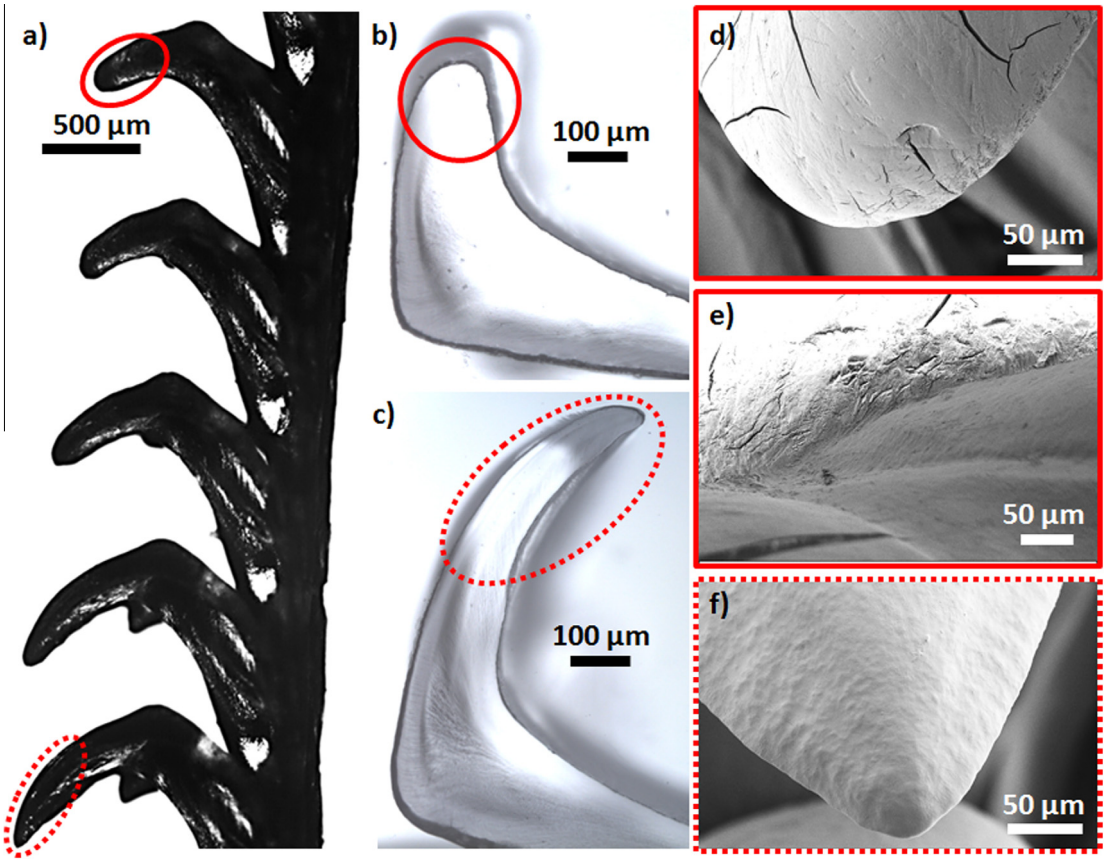

Fig. 9. (a) Optical micrograph of the major lateral tooth in the scraping and worn tooth developmental stage. (b and c) depict optical micrographs of longitudinal sections of an extensively worn versus a less worn tooth in the scraping region. (d and e) depict SEM images of a tip of a worn tooth. (f) SEM image of an intact mature tooth tip. The worn and intact tooth cusps are marked by full and dashed lines, respectively.

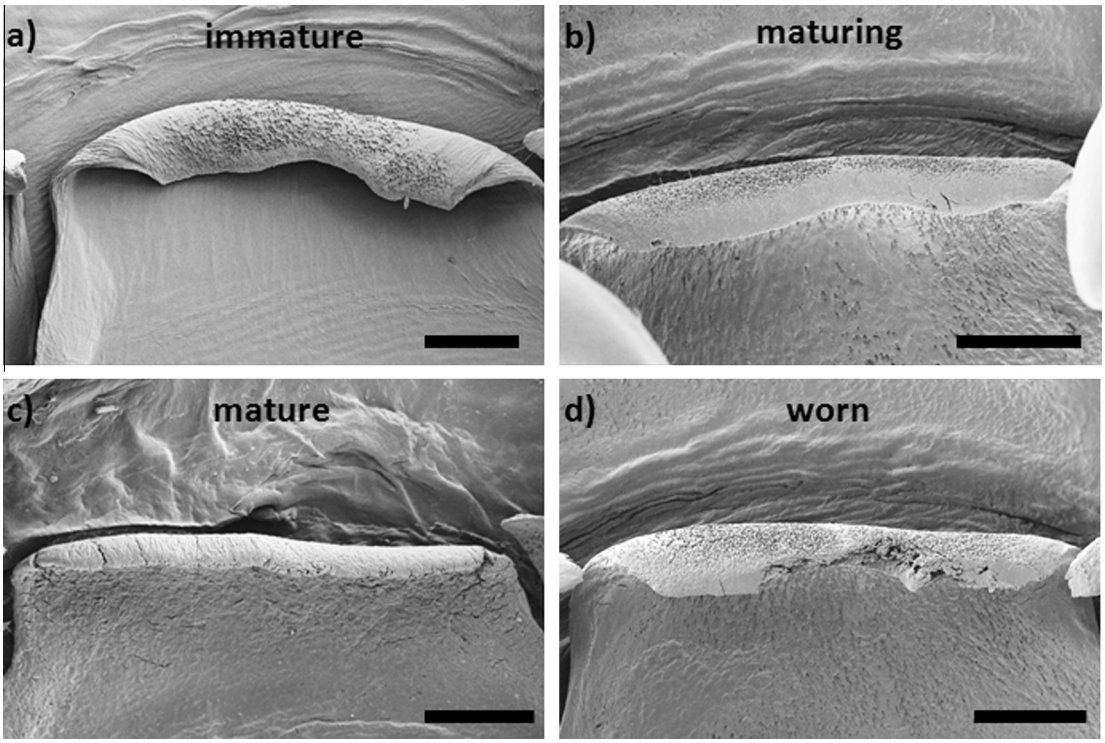

Fig. 10. (a–c) SEM micrographs of the large tooth in the immature, maturing and mature stages, respectively. (d) SEM micrograph of the central tooth in a late mature stage showing prominent signs of wear. Scale bar corresponds to 200 µm.

The typical rhipidoglossan radulae gastropods have numerous marginal teeth and can sweep and collect loosened material, including microalgae (Steneck and Watling, 1982). The major lateral teeth of these gastropods are soft and typically not mineralized with iron compounds (Goldberg, 2013; Steneck and Watling, 1982). The central tooth is assumed to be less involved in the feeding process (Fretter and Graham, 1962; Steneck and Watling, 1982). *Mcren* is an omnivorous rhipidoglossate, known to feed mostly on algae, complemented by tunicates (Beninger et al., 2001; Harris and Markl, 2000; Martin et al., 2011; Martin et al., 2007; Mazariegos-Villarreal et al., 2013; Morris et al., 1980). In contrast to typical rhipidoglossate gastropods, the dominant part of *Mcren's* diet consists of calcareous red algae, which are rather the typical food of doccoglossate limpets but is considered to be too hard for rhipidoglossan grazers (Steneck and Watling, 1982). We conclude therefore, that the radula of *Mcren* functions as a versatile harvest device that can withstand and remove the toughened cortical cells of these calcareous red algae as well as feed on much softer sources of nourishment. At this stage it is not yet clear how *Mcren* is able to tackle the task of consuming the hardened algal species. We note, however, that hardness alone is a bad descriptor of the excavating ability of radulae (Padilla, 1985).

The sophisticated harvesting apparatus of *Mcren* combines the ability of rhipidoglossane radula to successfully collect loosened small material with a surprisingly high ability to harvest hard algae, typical for doccoglossate limpets. Further studies are needed to further understand the high ability to harvest hard algae and the functional versatility and operation of the *Mcren* rhipidoglossan radula.

Acknowledgments

We thank J.C. Weaver (Wyss Institute for Biologically Inspired Engineering at Harvard University in Boston) for the initial sample preparation and stimulating discussions of the results. We also thank M. Schuchardt for her help in the initial analysis of μCT results, B. Schonert for sample embedding preparation, V. Reichel for helping with XRD measurement, S. Siegel and C. Li for help at the Synchrotron Beamline, and J. Steffen for helping with the sample preparation for AA analysis and ICP measurements. We gratefully acknowledge financial support from Max Planck Society. D. Faivre acknowledges support from the European Research Council (Starting Grant MB2 n°256915). P. Zaslansky is grateful for financial support of the German Research Foundation through SPP 1420.

References

Barber, A.H., Lu, D., Pugno, N.M., 2015. Extreme strength observed in limpet teeth. J. R. Soc. Interface 12.

Benecke, G., Wagermaier, W., Li, C., Schwartzkopf, M., Flucke, G., Hoerth, R., Zizak, I., Burghammer, M., Metwalli, E., Mueller-Buschbaum, P., Trebbin, M., Foerster, S., Paris, O., Roth, S.V., Fratzl, P., 2014. A customizable software for fast reduction and analysis of large X-ray scattering data sets: applications of the new DPDAK package to small-angle X-ray scattering and grazing-incidence small-angle X-ray scattering. J. Appl. Crystallogr. 47, 1797–1803.

Beninger, P.G., Cannuel, R., Blin, J.L., Pien, S., Richard, O., 2001. Reproductive characteristics of the archaeogastropod *Megathura crenulata*. J. Shellfish Res. 20, 301–307.

Cheng, S., Cetinkaya, M., Graeter, F., 2010. How sequence determines elasticity of disordered proteins. Biophys. J. 99, 3863–3869.

Cruz, R., Farina, M., 2005. Mineralization of major lateral teeth in the radula of a deep-sea hydrothermal vent limpet (Gastropoda: Neolepetopsidae). Mar. Biol. 147, 163–168.

Faivre, D., Ukmar Godec, T., 2015. From bacteria to mollusks: the principles underlying the biomineralization of iron oxide materials. Angew. Chem. Int. Ed. 54, 4728–4747.

Fretter, V., Graham, A., 1962. British Prosobranch Molluscs. Their Functional Anatomy and Ecology Ray Society Publication, London.

Goldberg, W.M., 2013. The Biology of Reefs and Reef Organisms. University of Chicago Press, Chicago.

Graham, A., 1973. Anatomical basis of function in buccal mass of prosobranch and amphineuran mollusks. J. Zool. 169, 317–348.

Grime, G.W., Watt, F., Mann, S., Perry, C.C., Webb, J., Williams, R.J.P., 1985. Biological applications of the Oxford scanning proton microprobe. Trends Biochem. Sci. 10, 6–10.

Guralnick, R., Smith, K., 1999. Historical and biomechanical analysis of integration and dissociation in molluscan feeding, with special emphasis on the true limpets (Patellogastropoda: Gastropoda). J. Morphol. 241, 175–195.

Harris, J.R., Markl, J., 2000. Keyhole limpet hemocyanin: molecular structure of a potent marine immunoactivator. Eur. Urol. 37, 24–33.

Isarankura, K., Runham, N.W., 1968. Studies on the replacement of the gastropod radula marking techniques colchicine prosobranchs pulmonates. Malacologia 7, 71–91.

Jones, E.I., McCance, R.A., Shackleton, L.R.B., 1935. The role of iron and silica in the structure of the radular teeth of certain marine molluscs. J. Exp. Biol. 12, 59–64.

Khanna, D.R., Yadav, P.R., 2004. Biology of Mollusca. Discovery Publishing House, New Delhi, India.

Killian, C.E., Metzler, R.A., Gong, Y., Churchill, T.H., Olson, I.C., Trubetskoy, V., Christensen, M.B., Fournelle, J.H., De Carlo, F., Cohen, S., Mahamid, J., Scholl, A., Young, A., Doran, A., Wilt, F.H., Coppersmith, S.N., Gilbert, P.U.P.A., 2011. Self-sharpening mechanism of the sea urchin tooth. Adv. Funct. Mater. 21, 682–690.

Kirschvink, J.L., Lowenstam, H.A., 1979. Mineralization and magnetization of chiton teeth: paleomagnetic, sedimentologic, and biological implications of organic magnetite. Earth Planet. Sci. Lett. 44, 193–204.

Lowenstam, H.A., 1962. Goethite in radular teeth of recent marine gastropods. Science 137, 279–280.

Lowenstam, H.A., 1971. Opal precipitation by marine gastropods (Mollusca). Science 171, 487–490.

Lowenstam, H.A., Weiner, S., 1989. On biomineralization. Oxford University Press, New York.

Lu, D., Barber, A.H., 2012. Optimized nanoscale composite behaviour in limpet teeth. J. R. Soc. Interface 9, 1318–1324.

Mann, S., Perry, C.C., Webb, J., Luke, B., Williams, R.J.P., 1986. Structure, morphology, composition and organization of biogenic minerals in limpet teeth. Proc. R. Soc. London, Ser. B Biol. Sci. 227, 179–190.

Martin, G.G., Martin, A., Tsai, W., Hafner, J.C., 2011. Production of digestive enzymes along the gut of the giant keyhole limpet *Megathura crenulata* (Mollusca: Vetigastropoda). Comp. Biochem. Physiol. A Mol. Integr. Physiol. 160, 365–373.

Martin, G.G., Oakes, C.T., Tousignant, H.R., Crabtree, H., Yamakawa, R., 2007. Structure and function of haemocytes in two marine gastropods, *Megathura crenulata* and *Aplysia californica*. J. Molluscan Stud. 73, 355–365.

Mazariegos-Villarreal, A., Pinon-Gimate, A.L., Aguilar-Mora, F., Medina, M., Serviere-Zaragoza, E., 2013. Diet of the Keyhole Limpet *Megathura Crenulata* (Mollusca: Gastropoda) in Subtropical Rocky Reefs. J. Shellfish Res. 32, 297–303.

Morris, R.H., Abbott, D.P., Haderlie, E.C., 1980. Prosobranchia: marine snails.

Padilla, D.K., 1985. Structural resistance of algae to herbivores – a biomechanical approach. Mar. Biol. 90, 103–109.

Paris, O., Li, C., Siegel, S., Weseloh, G., Emmerling, F., Riesemeier, H., Erko, A., Fratzl, P., 2007. A new experimental station for simultaneous X-ray microbeam scanning for small- and wide-angle scattering and fluorescence at BESSY II. J. Appl. Crystallogr. 40, S466–S470.

Rauscher, S., Baud, S., Miao, M., Keeley, F.W., Pomes, R., 2006. Proline and glycine control protein self-organization into elastomeric or amyloid fibrils. Structure 14, 1667–1676.

Rinkevich, B., 1993. Major primary stages of biomineralization in radular teeth of the limpet *Lottia gigantea*. Mar. Biol. 117, 269–277.

Rubin, D.J., Miserez, A., Waite, J.H., 2010. Diverse strategies of protein sclerotization in marine invertebrates: structure-property relationships in natural biomaterials. In: J. Casas, S.J. Simpson (Eds.), Advances in Insect Physiology: Insect Integument and Colour. pp. 75–133

Runham, N.W., 1962. The histochemistry of the radula of *Patella vulgata*. Q. J. Micros. Sci. 102, 371–380.

Runham, N.W., Thornton, P.R., Shaw, D.A., Wayte, R.C., 1969. Mineralization and hardness of radular teeth of the limpet *Patella Vulgata* L. Zeitschrift Fur Zellforschung Und Mikroskopische Anatomie 99, 608–626.

Rupley, J.A., 1964. The hydrolysis of chitin by concentrated hydrochloric acid, and the preparation of low-molecular-weight substrate for lysozyme. Biochim. Biophy. Acta (BBA) 83, 245–255.

Schindelin, J., Arganda-Carreras, I., Frise, E., Kaynig, V., Longair, M., Pietzsch, T., Preibisch, S., Rueden, C., Saalfeld, S., Schmid, B., Tinevez, J.-Y., White, D.J., Hartenstein, V., Eliceiri, K., Tomancak, P., Cardona, A., 2012. Fiji: an open-source platform for biological-image analysis. Nat. Methods 9, 676–682.

Seidel, R., Gourrier, A., Burghammer, M., Riekel, C., Jeronimidis, G., Paris, O., 2008. Mapping fibre orientation in complex-shaped biological systems with micrometre resolution by scanning X-ray microdiffraction. Micron 39, 198–205.

Shaw, J.A., Macey, D.J., Brooker, L.R., 2008. Radula synthesis by three species of iron mineralizing molluscs: production rate and elemental demand. J. Mar. Biol. Assoc. U.K. 88, 597–601.

Sone, E.D., Weiner, S., Addadi, L., 2005. Morphology of goethite crystals in developing limpet teeth: assessing biological control over mineral formation. Cryst. Growth Des. 5, 2131–2138.

Sone, E.D., Weiner, S., Addadi, L., 2007. Biomineralization of limpet teeth: a cryo-TEM study of the organic matrix and the onset of mineral deposition. J. Struct. Biol. 158, 428–444.

Steneck, R.S., Watling, L., 1982. Feeding capabilities and limitation of herbivorous molluscs: a functional group approach. Mar. Biol. 68, 299–319.

Towe, K.M., Lowenstam, H.A., 1967. Ultrastructure and development of iron mineralization in radular teeth of *Cryptochiton stelleri* (Mollusca). J. Ultrastruct. Res. 17, 1–13.

van der Wal, P., 1989. Structural and material design of mature mineralized radula teeth of *Patella vulgata* (gastropoda). J. Ultrastruct. Mol. Struct. Res. 102, 147–161.

van der Wal, P., Giesen, H.J., Videler, J.J., 2000. Radular teeth as models for the improvement of industrial cutting devices. Mater. Sci. Eng. C-Biomimetic Supramol. Syst. 7, 129–142.

Yang, Y.J., Jung, D., Yang, B., Hwang, B.H., Cha, H.J., 2014. Aquatic proteins with repetitive motifs provide insights to bioengineering of novel biomaterials. Biotechnol. J. 9, 1493–1502.